RESEARCH ARTICLE

Formulation and Evaluation of Nanoemulsion-Based Gels Containing Chrysophanol for Topical Fungal Treatment: A Quality by Design Approach

Kanchan Sanjivan Kakade*, Kiran Sanjay Bhise

MCES's Allana College of Pharmacy Pune, Maharashtra, India

Received: 5th Jun, 2025; Revised: 17th Jul, 2025; Accepted: 29th Jul, 2025; Available Online: 25th Sep, 2025

ABSTRACT

Fungal skin infections remain a clinical challenge and motivate development of alternative topical therapeutics. Chrysophanol, a natural anthraquinone, has limited cutaneous bioavailability, prompting formulation into nanocarriers to enhance delivery. In this study, Chrysophanol-loaded nanoemulsion (NE) and a corresponding nanogel were developed and optimized for dermal application. The optimized NE (F13) exhibited a mean droplet size of 231 nm, zeta potential −23 mV, and high entrapment efficiency (97.65 ± 0.35%). The nanogel displayed dermally acceptable pH (6.25 ± 0.11) and suitable rheology/spreadability. *In vitro* release studies confirmed sustained release (98.84 ± 2.59% from NE; 96.47 ± 2.96% from the nanogel). Functional evaluation was performed using *in vitro* antifungal enzyme inhibition assays targeting phospholipases and proteases. Relative to the pure extract, the NE increased inhibition to 61.37 ± 1.45% (phospholipase) and 55.29 ± 1.28% (protease), while the nanogel achieved 73.25 ± 1.62% and 69.84 ± 1.37%, respectively, approaching the standard ketoconazole (79.41 ± 1.18% and 74.92 ± 1.04%). These findings indicate that Chrysophanol nanocarriers improved enzyme-level antifungal activity while providing favorable physicochemical attributes for topical use, supporting their further development as promising natural antifungal formulations.

Keywords: Chrysophanol, NE, Nanogel, Antifungal therapy, Topical drug delivery, Quality by Design

How to cite this article: Kanchan Sanjivan Kakade, Kiran Sanjay Bhise. Formulation and Evaluation of Nanoemulsion-Based Gels Containing Chrysophanol for Topical Fungal Treatment: A Quality by Design Approach. International Journal of Drug Delivery Technology. 2025;15(3):1177-86. doi: 10.25258/ijddt.15.3.37

Source of support: Nil.

Conflict of interest: None

INTRODUCTION

Skin fungal infections represent a significant global public health issue, impacting millions of individuals each year. Dermatophytosis, candidiasis, and other superficial fungal infections cause discomfort, itching, and inflammation, and in severe cases, can lead to systemic complications, particularly in immunocompromised individuals[1-3]. Conventional antifungal agents, including azoles, allylamines, and polyenes, remain the cornerstone of treatment; however, their effectiveness is often compromised by drawbacks such as poor skin penetration, frequent dosing requirements, adverse effects, and the emergence of resistant fungal strains[4-6]. These limitations necessitate the exploration of alternative therapeutic strategies with improved efficacy, safety, and patient compliance. Chrysophanol, an anthraquinone derivative predominantly found in medicinal herbs such as *Rheum emodi* and *Cassia* species, has demonstrated diverse pharmacological activities, including antifungal, antibacterial, anti-inflammatory, and antioxidant properties. Chrysophanol has shown the ability to restrict fungal proliferation by compromising cell membrane integrity, altering fungal metabolism, and attenuating oxidative stress pathways[7-10]. Although its potential medicinal characteristics, the clinical use of Chrysophanol is constrained by its low water solubility, inadequate bioavailability, and restricted penetration across the skin barrier. These challenges highlight the need for novel formulation strategies that can enhance the solubility, stability, and skin penetration of Chrysophanol while ensuring sustained release at the target site.

Nanoemulsion (NE) based delivery methods are growing as a viable platform for enhancing the therapeutic efficacy of weakly soluble bioactives like Chrysophanol[11,12]. When incorporated into gels, NEs provide an additional benefit of enhanced viscosity, ease of application, and prolonged skin retention, making them particularly suitable for topical delivery systems[13-15].

Furthermore, the transparent and cosmetically acceptable appearance of NE-based gels improves patient compliance, which is crucial in long-term antifungal therapies. The integration of Quality by Design (QbD) principles into NE-based gel development for Chrysophanol delivery holds considerable promise[16-21]. Through systematic experimental design and risk assessment, a stable and efficacious NE-based gel of Chrysophanol can be developed to achieve superior antifungal activity, reduced dosing frequency, and improved patient adherence. Therefore, the present study is designed with the objective of formulating and evaluating NE-based gels containing Chrysophanol for topical treatment of fungal infections, employing a QbD approach.

**Author for Correspondence: kanchankakade10@gmail.com*

MATERIALS AND METHODS

Chrysophanol was obtained from Total Herb Solutions, India. All materials used in the investigation were of analytical quality and were obtained from Loba Chem Pvt. Ltd., Mumbai.

Physical Characterization and Drug-Excipients Compatibility Study

As part of the pre-formulation study, a preliminary physical inspection of Chrysophanol was carried out to assess its organoleptic properties. The evaluation primarily included observation of its appearance, colour, and taste, which serve as essential parameters for the preliminary identification and authentication of the drug. The UV analysis was performed to determine the λ-max of the drug by scanning 100 µg/mL of Chrysophanol methanolic solution between 200 to 400 nm[22-25]. FTIR spectra of Chrysophanol and physical mixture were recorded using an FTIR spectrometer (Version 7.03, Shimadzu, Japan) in the range of 4000–400 cm^{-1}.[26-29] The thermal behavior of Chrysophanol and physical mixture was investigated using a DSC (Mettler DSC 1 Star System, Mettler-Toledo, Switzerland) to assess its thermal stability and phase transitions[30,31].

Solubility Determination

The solubility of Chrysophanol was assessed in methanol, DMSO, and phosphate buffer at pH levels of 1.2, 6.8, and 7.4, maintained at 37 ± 0.5 °C. Excess drug was introduced to 10 mL of each solvent in glass vials, which were sealed with rubber stoppers and incubated in an orbital shaker at 37 ± 0.5 °C for 24 hours, thereafter, equilibrated for 12 hours in an incubator at the same temperature[32-34]. The solutions were subjected to filtration using a 0.45 µm Millipore filter, and the resulting filtrates were analyzed using UV spectrophotometry at λmax 276 nm[35,36]. Solubility was determined using the corresponding calibration curves.

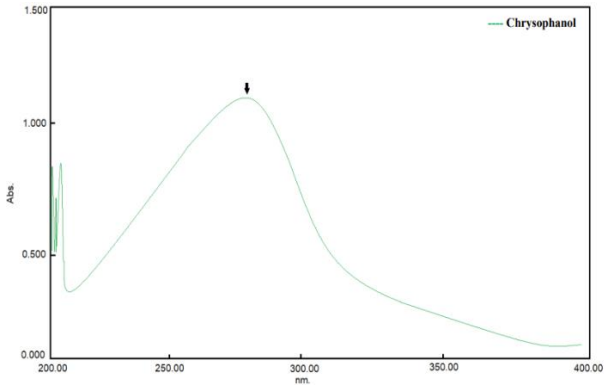

Figure 1: UV Spectrum of Chrysophanol in Methanol

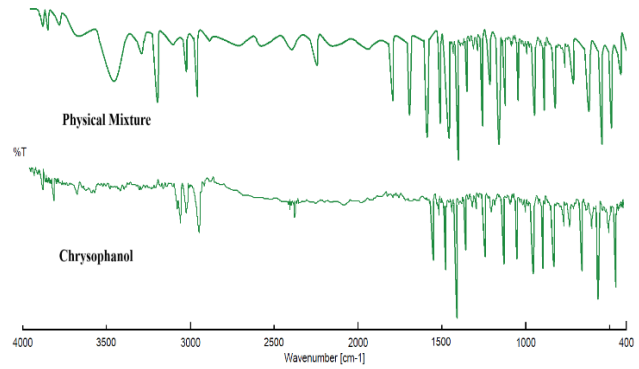

Figure 2: FTIR Spectra of Chrysophanol and Physical Mixture

Table 1: Independent Variables for QbD (SLD)

Independent Variables Coded Values	Low (-)	High (+)
X1: Concentrations of water (%)	62	64
X2: OO (%)	2	4
X3: Smix (%)	32	34

Screening of Oil, Surfactant and Co-surfactant (Solubility Study)

Solubility study was conducted to identify the oil, surfactant, and co-surfactant with the highest solubilizing capacity for poorly water-soluble Chrysophanol, a critical step in developing a stable and efficient delivery system. Biocompatible oils (almond, eucalyptus, and olive oil (OO)) were selected for their ability to dissolve lipophilic drugs, while surfactants (TW80, Span 20, Tween 20) and co-surfactants (PEG-400, ethanol, propylene glycol) were chosen for their emulsifying properties and suitable HLB values for NE or SNEDDS formulations. Samples were vortexed, equilibrated for 24 hours, and analyzed by UV spectroscopy at 276 nm to quantify Chrysophanol solubility. Excipients showing the highest solubility were considered optimal for enhancing drug loading, stability, and bioavailability, thus providing a rational basis for effective formulation development.

Preparation of Chrysophanol Loaded NE

14 formulations were selected for Chrysophanol-loaded NEs based on visual observations, including transparency and ZP, according to the factorial design. The necessary quantity of Chrysophanol was dissolved in the specified volume of the oil phase, thereafter including the preset Smix (surfactant and co-surfactant) and thoroughly mixing with a magnetic stirrer at ambient temperature. Double-distilled water was incrementally added until a clear, transparent NE was achieved, which was thereafter kept in sealed containers at room temperature.

Factorial Design

Construction of and Formula Optimization using SLD

A Simplex Lattice Design (SLD) was used. All variables explained in Table 1.

TW80:TP (Smix) was combined in different quantities with Olive Oil (OO) to get the OO:Smix (TW80:TP) ratios shown in Tables 2 and 3. The optimisation of N-NEs was conducted using Design-Expert (Stat-Ease Inc., USA), with

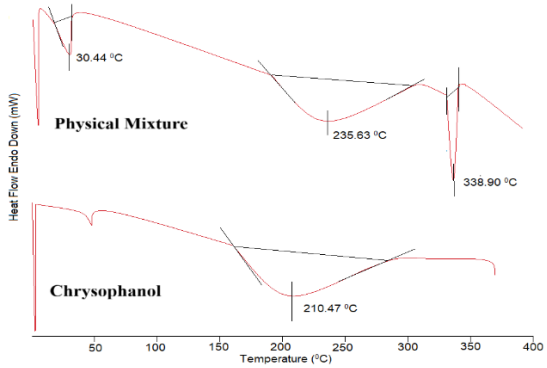

Figure 3: DSC Spectra of Chrysophanol and Physical Mixture

water concentration (X1), OO (X2), and Smix (X3) as independent factors, and particle size (Y1) and ZP (Y2) as dependent responses. Statistical correlations among variables and three-dimensional response surface plots were produced, with the factorial design layout shown in Tables 2 and 3.

Characterization of NE

The prepared NE formulations were subjected to preliminary physical evaluation. They were carefully inspected visually for their color, transparency, homogeneity, and consistency in order to assess their overall appearance and stability. Average droplet size and size distribution of the NE were assessed by photon correlation spectroscopy (PCS), which quantifies the variations in light scattering intensity resulting from the Brownian motion of dispersed droplets. The study was conducted using a Zetasizer (1000 HS, Malvern Instruments, Italy), a highly sensitive device often used for particle size characterization. The zeta potential (ZP) of a droplet denotes the total surface charge that the particle attains in a certain dispersion medium. The pH of the prepared NE formulations was determined at 25 °C using a calibrated digital pH meter. The surface morphology of the synthesized NE was examined via SEM and TEM analysis.

In-vitro Release Study of Chrysophanol Loaded Nano-emulsion Formulations

The *in vitro* drug permeation study was conducted using a Franz diffusion cell fitted with a dialysis membrane to simulate drug release across a semi-permeable barrier.

Accelerated Stability Study

Stability experiments were performed following the ICH requirements over a three-month period to evaluate the adaptability of the optimized NE formulation.

Preparation of Gel from NE

An adequate quantity of carbopol 940 (3% solution) was incorporated into the previously produced NEs and stirred for about thirty minutes. This resulted in the creation of nanogel.

Characterization of Nanogel

The pH values of the formulated nanogels were measured at 25 °C using a calibrated digital pH meter. The viscosities of the formulated nanogels were measured at 25 °C using a Brookfield DV-E viscometer (Brookfield Engineering Laboratories, USA). The drug content in the nanogel was quantified using a UV–Visible spectrophotometer. Absorbance was measured at 276 nm, and drug content was calculated using the standard calibration curve of Chrysophanol. Spreadability of nanogel was determined. The *in vitro* drug permeation study was carried out using a Franz diffusion cell fitted with a dialysis membrane to simulate transdermal drug delivery. The system was then operated under controlled experimental conditions to monitor the release and permeation of the encapsulated drug over a predetermined time period.

Accelerated Stability Study

The stability experiments were conducted for optimized nanogel formulation in compliance with ICH recommendations for a period of three months.

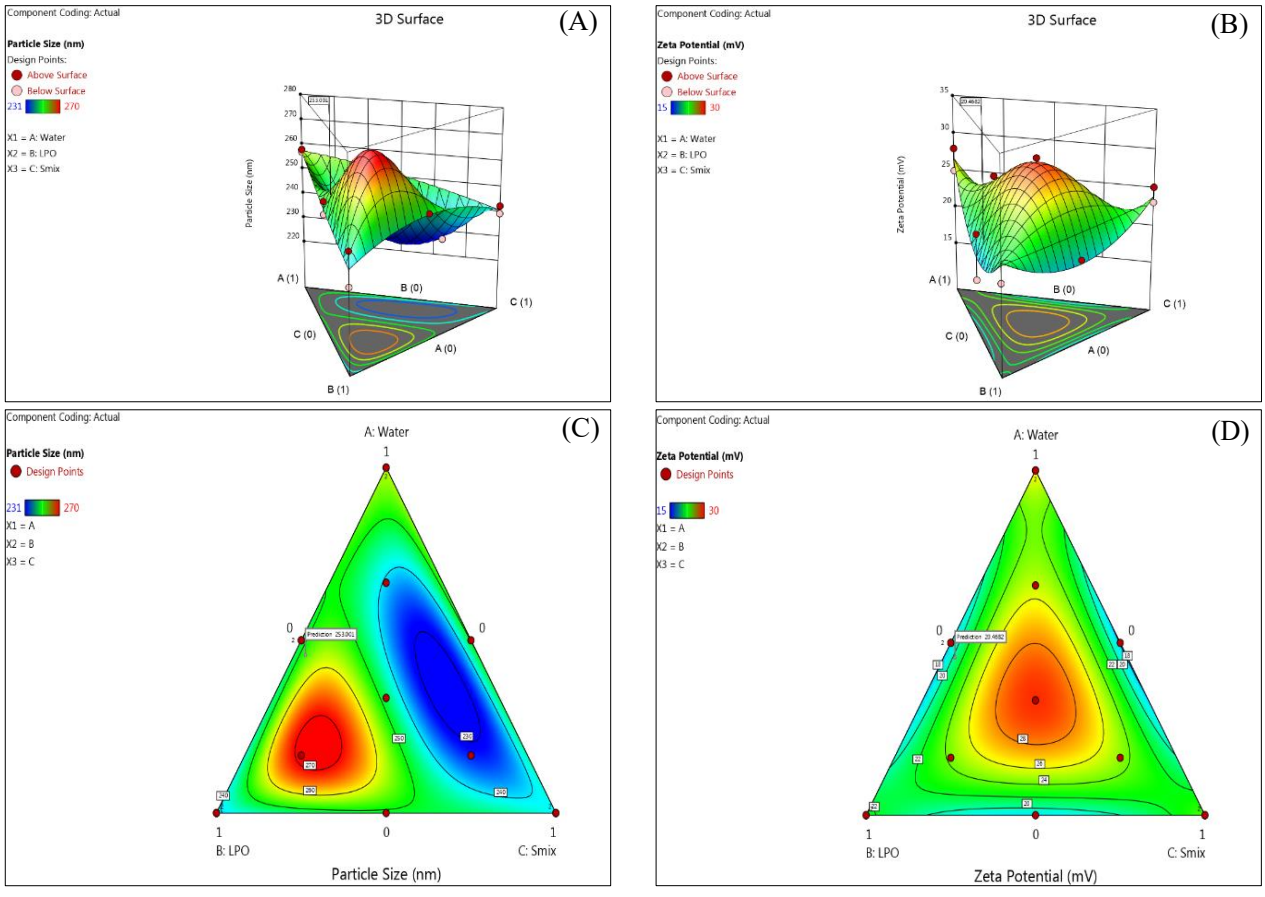

Figure 4: Response surface plots for X1, X2 and X3 on (A) Mean Particle Size (Y1); (B) ZP (Y2); and contour plots for (C) Mean Particle Size (Y1); (D) ZP (Y2)

Table 2: Experimental levels of independent variables used for optimization

Batch Code	X1: Water (%)	X2: OO (%)	X3: Smix (%)	Batch Code	X1: Water (%)	X2: OO (%)	X3: Smix (%)
F-1	0.5	0	0.5	F-8	0	1	0
F-2	0.5	0.5	0	F-9	0.5	0.5	0
F-3	0.333333	0.333333	0.333333	F-10	0	0	1
F-4	1	0	0	F-11	0	0	1
F-5	0.666667	0.166667	0.166667	F-12	0	0.5	0.5
F-6	1	0	0	F-13	0.166667	0.166667	0.666667
F-7	0.166667	0.666667	0.166667	F-14	0	1	0

Table 3: Experimental layout based on Simplex Lattice Design (SLD)

Batch Code	F-1	F-2	F-3	F-4	F-5	F-6	F-7	F-8	F-9	F-10	F-11	F-12	F-13	F-14
X1: Water (%)	62	64	66	63	62.21	63	62.36	62	63.56	64	62.21	62	62	62
X2: OO (%)	2	2	2	2	2.64	2	1.32	2	0.64	2	0.64	2	4	4
X3: S_{mix} (%)	34	32	32	33	32.16	32	32.64	34	32.16	32	33.56	33	32	32
Particle Size (nm)	251	250	249	257	238	258	270	246	245	239	242	249	231	233
ZP (mV)	18	15	30	28	-26	-25	24	20	21	23	25	19	-23	25

Table 4: Solubility study in different solvents

Solvent	Observed Solubility (µg/ml)
Methanol	48.08 ± 0.32
DMSO	55.25 ± 0.51
pH buffer 1.2	08.16 ± 0.23
pH buffer 6.8	52.36 ± 0.14
pH buffer 7.4	65.25 ± 0.19

Table 5: Solubility of Chrysophanol

Name of Excipients	Solubility (mg/ml)	Name of Excipients	Solubility (mg/ml)
OO	46.48±0.3	TW80	39.02±0.2
Eucalyptus Oil,	27.56±0.9	PEG-400	35.58±0.5
Almond Oil,	28.38±0.11	---	---

In-vitro Antifungal Enzyme Assay

The antifungal enzyme inhibitory activity of Chrysophanol formulations was evaluated using *in vitro* assays targeting extracellular phospholipases and proteases, which are key virulence factors of pathogenic fungi. A 0.5 mL aliquot of each sample—control (untreated), standard (ketoconazole, 20 µg/mL), pure Chrysophanol extract, optimized Chrysophanol nanoemulsion (F13), and Chrysophanol nanogel—was incubated with equal volumes of substrate solution in phosphate buffer (pH 7.0). For the phospholipase assay, egg yolk phosphatidylcholine (2 mg/mL) was used as the substrate, while for the protease assay, bovine serum albumin (2 mg/mL) served as the substrate.

The mixtures were incubated at 37 °C for 30 minutes. Enzyme activity was quantified by measuring the release of free amino groups (protease assay) or free fatty acids (phospholipase assay) spectrophotometrically.

Enzyme inhibition (%) was calculated relative to the control using the formula:

$$\%\ Inhibition = \frac{\mathrm{A(control)} - \mathrm{A(sample)}}{\mathrm{A(control)}} \times 100$$

where $A_{control}$ is the absorbance of the enzyme reaction without inhibitor, and A_{sample} is the absorbance in the presence of test formulations. All experiments were performed in triplicate, and mean values were recorded.

RESULTS AND DISCUSSION

UV-Visible Spectroscopy

Wavelength of maximum absorption (λmax) of Chrysophanol was established at 276 nm in methanol, signifying its pronounced π–π* electronic transitions typical of its conjugated aromatic structure. The absorption maximum used as a reference for subsequent spectrophotometric analyses and quantification tests (Figure 1).

Drug-Excipients Compatibility Study

FTIR Analysis

The FTIR spectra of Chrysophanol and the physical mixture of excipients (Pectin, Tween-80, PEG-400, and Carbopol 980) (Figure 2). No significant shifts were noted between the spectra of the pure drug and the physical mixture, indicating the absence of chemical interactions. All functional group peaks of Chrysophanol remained intact in the formulation, confirming its compatibility with the excipients.

DSC

DSC analysis revealed the thermal behavior of Chrysophanol and its compatibility with selected excipients. Pure Chrysophanol exhibited a sharp endothermic peak at 159.99 °C, corresponding to its melting point and crystalline nature. In 1:1 physical mixture with Chrysophanol, these peaks were retained without significant shifts, disappearance, or new peak formation, indicating no chemical or physical interactions. Thus, the DSC results confirm that Chrysophanol is thermally compatible with Pectin, TW80, and Carbopol 980, supporting their suitability for formulation development (Figure 3).

Solubility Determination

The solubility of Chrysophanol was systematically evaluated in a range of solvents, including Methanol, DMSO, and various buffer solutions, maintained at a controlled temperature of 37 ± 0.5 °C to mimic physiological conditions. The solubility data obtained from these studies are summarized in Table 4, providing essential information for the selection of suitable solvents in subsequent formulation and analytical procedures.

Table 6: Results of Analysis of Variance for Measured Response (Particle Size)

Parameters	Values	
	Particle Size	Zeta Potential
Model	Special Quartic model (Significant)	Special Cubic model (Significant)
Model p-value	0.0206	0.0273
Standard Deviation	4.69	2.42
F-Value	7.40	4.94
CV	1.90%	10.50%
R^2	0.9221	0.8091
Adequate Precision	10.3807	6.7562
Regression Equation	Y1 = 257.40 X1 + 239.40 X2 + 240.40 X3 – 4.39 X1 X2 + 6.82 X1 X3 + 34.82 X2 X3 - 1399.80$X1^2X2X3$+2776.20$X1X2^2X3$-1590.71$X1X2X3^2$	Y1 = 26.63 X1 + 22.49 X2 + 23.77 X3 – 25.76 X1 X2 – 29.59 X1 X3 - 18.45X2 X3 + 357.67X1X2X3

Table 7: Characterization of NE

Formulation code	pH value of NE	Viscosity (cps)	Formulation code	pH value of NE	Viscosity (cps)
F1	5.92 ± 0.02	1331 ± 2.33	F8	6.57 ± 0.04	1651 ± 2.39
F2	5.54 ± 0.03	1430 ± 2.28	F9	5.58 ± 0.06	1709 ± 2.33
F3	5.55 ± 0.04	1575 ± 2.21	F10	6.93 ± 0.03	1845 ± 2.27
F4	6.98 ± 0.01	1721 ± 2.29	F11	5.56 ± 0.02	1525 ± 2.26
F5	5.12 ± 0.03	1581 ± 2.31	F12	6.48 ± 0.04	1765 ± 2.21
F6	5.93 ± 0.02	1625 ± 2.35	F13	5.29 ± 0.05	1875 ± 2.28
F7	5.45 ± 0.01	1535 ± 2.36	F14	6.69 ± 0.03	1678 ± 2.31

Table 8: Characterization of NE

Formulation code	Drug Content (%)	Formulation code	Drug Content (%)
F1	87.19 ± 0.27%	F8	95.47 ± 0.32%
F2	86.91 ± 0.29%	F9	92.21 ± 0.31%
F3	87.92 ± 0.30%	F10	94.38 ± 0.30%
F4	85.38 ± 0.31%	F11	92.36 ± 0.28%
F5	94.91 ± 0.32%	F12	93.38 ± 0.29%
F6	92.28 ± 0.26%	F13	97.65 ± 0.35%
F7	93.38 ± 0.28%	F14	94.35 ± 0.39%

Screening of Oil, Surfactant and Co-surfactant (Solubility Study)

Oils, surfactants, and co-surfactants were screened for their solubility of Chrysophanol (Table 5). OO was selected as the oil phase for its superior solubilizing capacity, TW80 as the surfactant due to its excellent emulsifying ability, and PEG-400 as the co-surfactant to enhance solubility and formulation stability. This systematic selection ensured optimal drug incorporation and supported the development of a stable, effective NE.

Formulation and Selection of NE

Based on careful visual evaluation, including parameters such as clarity, transparency, and pH, a total of 14 formulations were systematically selected according to the factorial design for the development of Chrysophanol-loaded NEs.

These selected formulations were further optimized to ensure stability, uniformity, and suitability for topical application.

Formulation Design

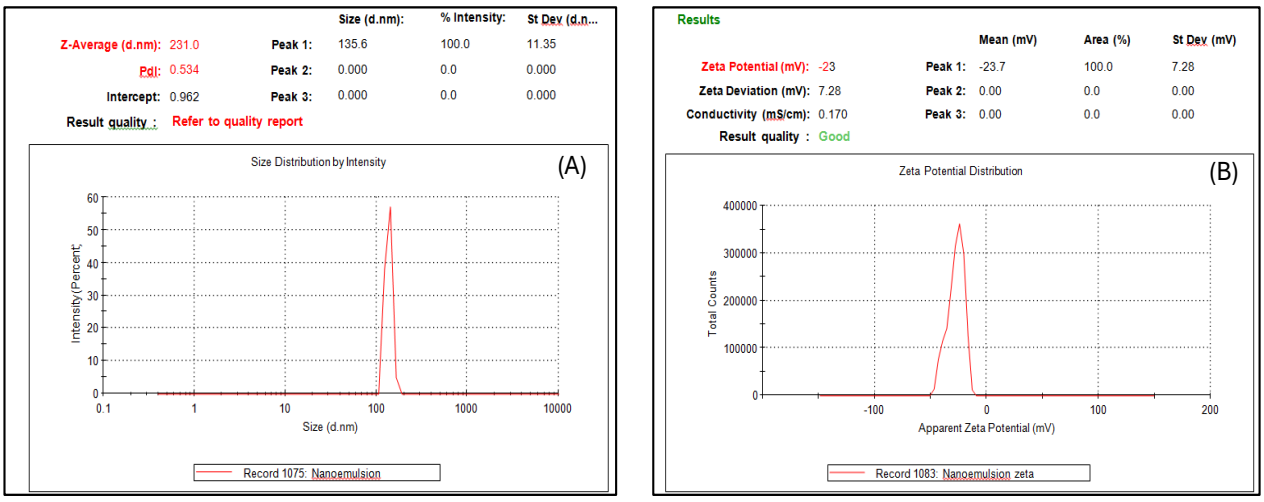

Figure 5: (A) Particle size and (B) ZP of F13 formulation

Table 1 presents the two components in their lower, middle, and higher levels in both coded and uncoded formats. The responses Y1 and Y2 ranged from 231 to 270 d.nm and from 15 to 30 mV, respectively. The nine formulations were analysed using a main effects model, identified as the optimal match for both responses using Design Expert® software. The regression equations, together with R^2, standard deviation, and coefficient of variation percentages, are shown in Table 6. The ANOVA findings validated the statistical significance of the model for all dependent variables. The independent variables X1, X2, and X3 favourably influenced the zeta potential while facilitating the target particle size in the NE formulation.

Model Assessment

The data were analysed using Design Expert® software, which recommended the Main Effects Model for all replies. Statistical analysis was conducted using ANOVA, with findings shown in Table 6. Regression coefficients with numerous factor terms indicate interactions, demonstrating that the connection between variables and responses is not purely linear. When several elements are altered concurrently at distinct levels in a formulation, each component might affect the reaction to differing extents.

Response Surface Plot Analysis

The particle size of polymeric nanoparticles (PNs) is a critical parameter influencing drug release and absorption, with smaller particles providing a larger surface area and improved bioavailability. The PDI accounts for the mean particle size, solvent refractive index, measurement angle, and distribution variance. Low PDI indicates a homogeneous particle population, while high PDI suggests a broad or multiple size distributions. Based on the 3D response surface plot (Figure 4 A), the formulation batch with the smallest particle size is preferred as the optimized batch. Batch F13, containing 32% Smix and 4% OO, exhibited an optimized particle size of 231 nm. Zeta potential (ZP) is a key determinant of NE stability, reflecting the surface charge of dispersed droplets. High absolute ZP values generate strong electrostatic repulsion, preventing droplet aggregation and phase separation. Typically, a ZP around ±30 mV is considered optimal for long-term stability, counteracting attractive forces such as van der Waals and hydrophobic interactions. Controlling ZP enhances physical stability, dispersion, bioavailability, and shelf life of NEs. Analysis of the 3D response surface plot (Figure 4 B) and regression coefficients indicated that ZP increases with higher OO concentration, with no significant interaction or nonlinearity observed, highlighting OO as the primary factor affecting ZP.

Figures 4C and 4D show contour plots in the QbD approach, illustrating the relationship between CQAs and CPPs. The flat contours indicate that the CQAs are relatively insensitive to variations in the corresponding CPPs within this region, suggesting a robust design space. Both responses demonstrate optimized outcomes within the defined design space.

Characterization of NE

Physical Characterization

All the prepared formulations appeared clear, transparent, and homogeneous, exhibiting a smooth texture without any signs of grittiness or particle aggregation. No clogging was observed, and the formulations demonstrated an appropriate and uniform consistency suitable for their intended application.

Droplet Size and Size Distribution

The particle size of PNs considerably influences medication release and absorption, since smaller particles provide an increased surface area that improves bioavailability (Figure 5 A). The optimized formulation (F13) exhibited a mean particle size of 231 nm and a polydispersity index (PDI) of 0.534.

ZP Analysis

The ZP of the drug-loaded NE was determined to be –23 mV (Figure 5 B). Such a pronounced negative charge suggests substantial electrostatic repulsion among the droplets, enhancing the NE's physical stability by minimizing the risk of aggregation and coalescence over time.

Surface Morphological Study

The micrographs revealed that the NE droplets possessed smooth and uniform surfaces, indicating the absence of aggregation or irregularities. Additionally, the droplets exhibited a predominantly spherical shape with an average particle size of approximately 200 nm, suggesting a well-controlled formulation and nanoscale dispersion. SEM and TEM image of F13 formulation are shown in Figure 6.

Measurement of pH

The pH values of the selected NE (NE) formulations (F1–F14) were observed to range between 5.12 and 6.98, as presented in Table 7.

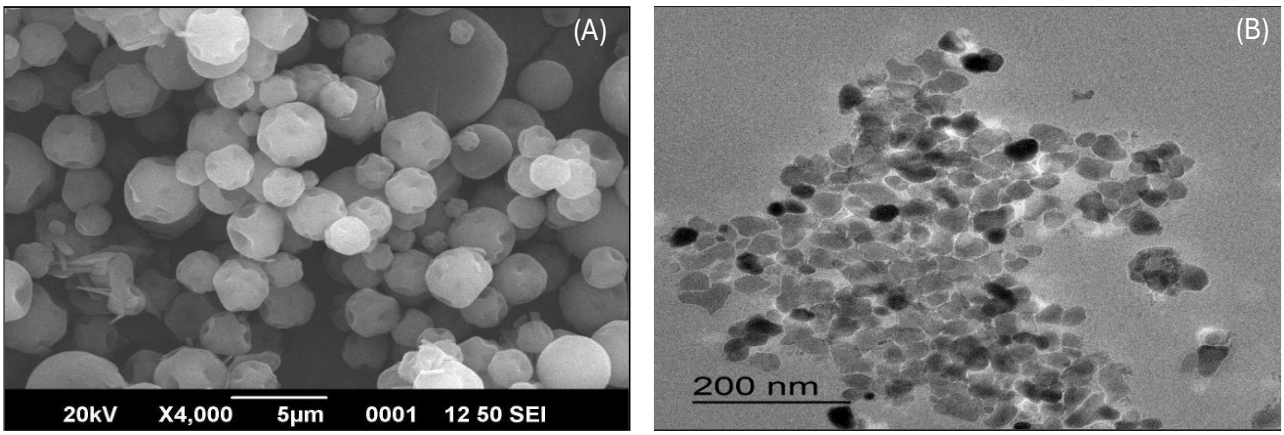

Figure 6: (A) SEM and (B) TEM image of F13 formulation

Table 9: *In-vitro* release profile of Nano-emulsion

Time (min)	Pure Drug Solution	Nano-emulsion (F13)	Time (min)	Pure Drug Solution	Nano-emulsion (F13)
60	17.48 ± 1.36	16.24 ± 1.59	300	-	75.02 ± 2.61
120	52.36 ± 2.41	22.04 ± 2.18	360	-	87.24 ± 2.60
180	70.65 ± 1.69	37.62 ± 1.91	420	-	92.02 ± 2.55
240	98.36 ± 2.32	54.52 ± 2.21	480	-	98.84 ± 2.59

Table 10: Stability study of parameters of the optimized formulation (F13)

Parameters	Initial Month	1st Month	2nd Month	3rd Month
pH	5.29 ± 0.05	5.41 ± 0.04	5.39 ± 0.02	5.33 ± 0.03
Viscosity (cps)	1515 ± 2.29	1525 ± 2.28	1555 ± 2.33	1519 ± 2.30
Drug content (%)	97.65 ± 0.35	97.23 ± 0.35	97.89 ± 0.31	98.00 ± 0.39

These values fall well within the normal physiological pH range of human skin (5.0–7.0), indicating that the formulations are likely to be non-irritating and compatible with topical application.

Measurement of Viscosity

All formulations exhibited a shear-thinning behavior, indicating that their viscosity decreased progressively with an increase in applied shear stress, a desirable property for topical applications. Among the tested formulations, F13 demonstrated the highest viscosity, suggesting superior structural stability and optimal consistency compared to the other formulations.

Drug Content of NE

To accurately quantify the encapsulated drug, the drug content was determined and the results indicated that the percentage of drug content in the NE ranged from 85.33% to 97.65%, as summarized in Table 8. These values demonstrate that the drug content of all formulations remained within the acceptable and permissible limits.

In-vitro Release Study

Batch F13 had the largest release, about 98.84 ± 2.59% (Table 9 and Figure 7). An initial burst release was seen,

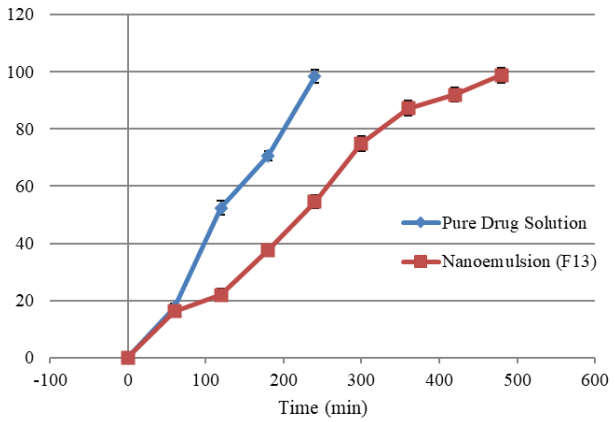

Figure 7: *In-vitro* drug release study of F13

Table 11: Characterization of Nanogel

S. No.	Formulation code	pH value of NE gel	Viscosity (cps)
1	F13	6.25 ± 0.11	1811 ± 1.36

Table 12: Characterization of NE Gel

S. No.	Formulation code	Drug Content (%)	Spreadability (%)
1	F13	93.36 ± 0.14%	94.49 ± 1.09%

Table 13: *In-vitro* release profile of Nanogel

Time (Hours)	Nanogel (F13)	Time (Hours)	Nanogel (F13)
0	0	8	78.28 ± 2.32
2	14.41 ± 1.36	10	88.29 ± 2.56
4	28.23 ± 2.41	12	96.47 ± 2.96
6	55.58 ± 1.69	---	---

Table 14: Stability study of parameters of the optimized formulation (F13)

Parameters	Initial Month	1st Month	2nd Month	3rd Month
pH	6.25 ± 0.11	6.79 ± 0.14	6.89 ± 0.12	6.81 ± 0.13
Viscosity (cps)	1811 ± 1.36	1827 ± 1.20	1847 ± 1.39	1796 ± 1.14
Drug content (%)	93.36 ± 0.14	93.35 ± 0.25	92.93 ± 0.13	93.40 ± 0.26

probably because to the tiny particle size offering an extensive surface area, together with the fast diffusion of the drug from the emulsion's outer shell.

Accelerated Stability Study

The optimized NE was subjected to comprehensive stability studies, and the outcomes are presented in Table 10. The results indicate that the Chrysophanol-loaded NE (Formulation batch F13) maintained its physicochemical integrity under the specified temperature and humidity conditions.

Characterization of NE Gel

Measurement of pH and Viscosity

The pH of the optimized NE (NE) and its corresponding gel formulation (F13) was measured and found to be 6.25 ± 0.11, as presented in Table 11. Therefore, the developed NE and its nanogel formulation can be considered suitable and safe for topical application, providing a promising platform for effective skin delivery of the active compound. Among the tested formulations, F13 demonstrated the highest viscosity, suggesting a more structured gel network, as summarized in Table 11.

Drug Content of Nanogel

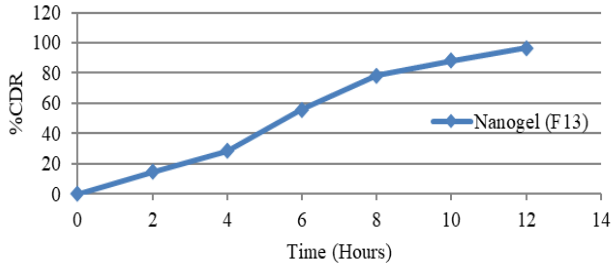

Figure 8: *In-vitro* drug release study of F13 formulation

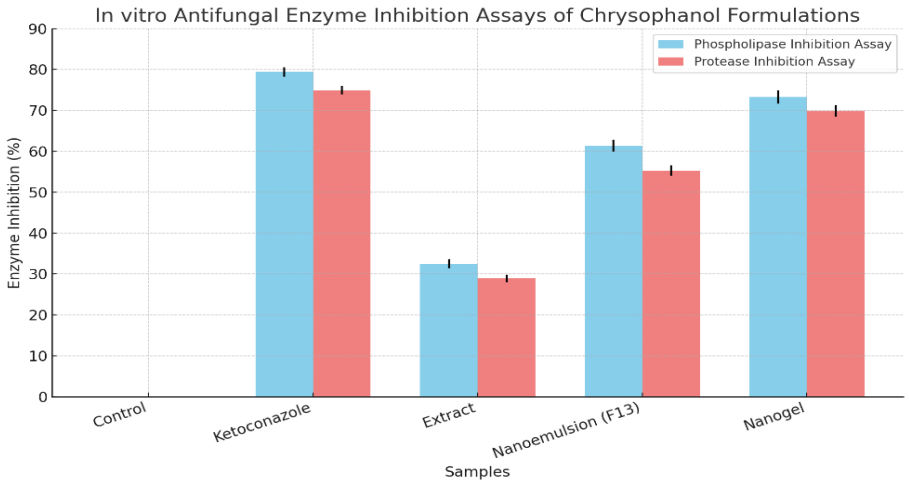

Figure 9: *In vitro* antifungal enzyme inhibition assay

The drug content in the nanogel, prepared by incorporating a gelling agent into the NE, may slightly decrease due to the volume occupied by the swollen gelling agent. It was determined using a UV spectrophotometer at 276 nm. The drug content of the nanogel was 93.36% (Table 12), which falls within the acceptable range for the formulations.

Spreadability

Among the tested formulations, F13 exhibited excellent spreadability, indicating its potential for uniform application and better patient compliance, as summarized in Table 12.

In-vitro Release Study

The maximum release observed for F13 was 96.47 ± 2.96% (Table 13 and Figure 8). An initial burst release was noted, likely due to the small particle size increasing the gel's surface area, along with diffusion of the drug from the gel's outer layer.

Accelerated Stability Study

The optimized nanogel formulations were subjected to comprehensive stability studies, and the findings are summarized in Table 14. The results indicate that the Chrysophanol-loaded NE gels, particularly formulation batch F15, exhibited excellent stability under the specified temperature and humidity conditions.

In-vitro Antifungal Assay

The control enzyme reactions exhibited maximum activity in the absence of inhibitors (Figure 9). The pure Chrysophanol produced moderate inhibition of phospholipase (32.46 ± 1.12%) and protease (28.91 ± 0.94%) activity. The optimized nanoemulsion (F13) demonstrated significantly higher inhibition, with values of 61.37 ± 1.45% for phospholipase and 55.29 ± 1.28% for protease. The nanogel formulation further enhanced activity, inhibiting 73.25 ± 1.62% of phospholipase and 69.84 ± 1.37% of protease activity. These results were comparable to the standard ketoconazole, which achieved 79.41 ± 1.18% inhibition of phospholipase and 74.92 ± 1.04% inhibition of protease. The enzyme inhibition assays clearly demonstrated that Chrysophanol formulations were capable of suppressing fungal virulence enzymes, which play a pivotal role in tissue invasion and pathogenicity. While the pure Chrysophanol showed only modest inhibition, incorporation into nanoemulsion significantly improved enzyme suppression, likely due to enhanced solubility and better interaction of Chrysophanol with enzyme active sites. The nanogel formulation provided the highest inhibition, which may be attributed to its sustained release and greater bioavailability on the enzyme–substrate interface. Importantly, the nanogel's inhibition values were statistically comparable to those of ketoconazole, suggesting that Chrysophanol, when delivered via nanocarrier systems, could serve as a promising natural alternative in antifungal therapy.

CONCLUSION

This study demonstrated the successful development of Chrysophanol-loaded nanoemulsion and nanogel formulations with properties suitable for topical application. The nanocarrier systems enhanced the stability, release characteristics, and dermal compatibility of Chrysophanol. Importantly, *in vitro* enzyme inhibition assays revealed that incorporation into nanoemulsion and gel systems markedly improved the ability of Chrysophanol to suppress fungal virulence enzymes such as phospholipases and proteases. Among the formulations, the nanogel exhibited superior inhibitory activity, approaching that of the standard antifungal drug. These findings highlight the potential of Chrysophanol nanocarriers as effective natural alternatives for topical antifungal therapy. Future investigations should extend to antifungal growth assays, skin permeation studies, and *in vivo* evaluations to confirm the therapeutic applicability of these formulations.

Acknowledgements

The author expresses sincere gratitude to Dr. Kiran S. Bhise, Principal and Research Guide, Allana College of Pharmacy, Pune, for her valuable guidance and support throughout this work. The author also acknowledges Allana College of Pharmacy, Pune, and its library facilities for providing access to research articles and journals that significantly contributed to this study.

REFERENCES

1. Corzo-León DE, Munro CA, MacCallum DM. An *ex vivo* human skin model to study superficial fungal infections. Front Microbiol. 2019;10(JUN).

2. Hay R. Therapy of skin, hair and nail fungal infections. J Fungi. 2018;4(3).
3. Verma S, Utreja P. Vesicular nanocarrier based treatment of skin fungal infections: Potential and emerging trends in nanoscale pharmacotherapy. Asian J Pharm Sci. 2019;14(2):117–29.
4. Garg A, Sharma GS, Goyal AK, Ghosh G, Si SC, Rath G. Recent advances in topical carriers of anti-fungal agents. Heliyon. 2020;6(8).
5. Hur MS, Park M, Jung WH, Lee YW. Evaluation of drug susceptibility test for Efinaconazole compared with conventional antifungal agents. Mycoses. 2019;62(3):291–7.
6. Yassin MT, Elgorban AM, Al-Askar AA, Sholkamy EN, Ameen F, Maniah K. Synergistic Anticandidal Activities of Greenly Synthesized ZnO Nanomaterials with Commercial Antifungal Agents against Candidal Infections. Micromachines. 2023;14(1).
7. Seo EJ, Ngoc TM, Lee SM, Kim YS, Jung YS. Chrysophanol-8-O-glucoside, an anthraquinone derivative in rhubarb, has antiplatelet and anticoagulant activities. J Pharmacol Sci. 2012;118(2):245–54.
8. Deitersen J, El-Kashef DH, Proksch P, Stork B. Anthraquinones and autophagy – Three rings to rule them all? Bioorganic Med Chem. 2019;27(20).
9. Park DB, Park BS, Kang HM, Kim JH, Kim IR. Chrysophanol-Induced Autophagy Disrupts Apoptosis via the PI3K/Akt/mTOR Pathway in Oral Squamous Cell Carcinoma Cells. Med. 2023;59(1).
10. Prateeksha, Yusuf MA, Singh BN, Sudheer S, Kharwar RN, Siddiqui S, et al. Chrysophanol: A natural anthraquinone with multifaceted biotherapeutic potential. Biomolecules. 2019;9(2).
11. Zhang G, Li J, Lv H, Qian C, Li X, Yang Z, et al. Comparative pharmacokinetics of rhubarb anthraquinones loaded nanoemulsion by different plasma drug concentration calculation methods. Acta Pol Pharm - Drug Res. 2021;78(4):475–83.
12. Nasiri MI, Vora LK, Ershaid JA, Peng K, Tekko IA, Donnelly RF. Nanoemulsion-based dissolving microneedle arrays for enhanced intradermal and transdermal delivery. Drug Deliv Transl Res. 2022;12(4):881–96.
13. Latif MS, Nawaz A, Asmari M, Uddin J, Ullah H, Ahmad S. Formulation Development and *In Vitro/In Vivo* Characterization of Methotrexate-Loaded Nanoemulsion Gel Formulations for Enhanced Topical Delivery. Gels. 2023;9(1).
14. Alqarni MH, Foudah AI, Aodah AH, Alkholifi FK, Salkini MA, Alam A. Caraway Nanoemulsion Gel: A Potential Antibacterial Treatment against Escherichia coli and Staphylococcus aureus. Gels. 2023;9(3).
15. Prohit PV, Pakhare PS, Pawar VB, Dandade SS, Waghmare MS, Shaikh FA, et al. Formulation and Comparative Evaluation of Naproxen-Based Transdermal Gels. J Pharm Sci Comput Chem. 2025;1(2):83–105.
16. Özcan S, Levent S, Can NÖ. Quality by design approach with design of experiment for sample preparation techniques. Adv Sample Prep. 2023;7.
17. Sangshetti JN, Deshpande M, Zaheer Z, Shinde DB, Arote R. Quality by design approach: Regulatory need. Arab J Chem. 2017;10:S3412–25.
18. Khanahmadi M, Shahrezaei F, Sharifi M, Rezanejade Bardajee G. Ultrasound-Assisted Preparation and Optimization of Natural Flavoring Nanoemulsion for Dairy Products Based on Pistacia Khinjuk in Lab Scale. Chem Methodol. 2023;7(7):524–39.
19. Kumar RR, Krishnan K, Sankararao G, Samathoti P, Kumar JP, Bagade OM, et al. Biochemical Engineering of Green Nanomaterials for Targeted Drug Delivery and Therapeutic Applications. J Chem Rev. 2025;6(3):191–215.
20. Reddy KTK, Dharmamoorthy G, Devi DV, Vidiyala N, Bagade OM, Elumalai S, et al. Phytoconstituent-Based Green Synthesis of Nanoparticles: Sources and Biomedical Applications in Cancer Therapy. Asian J Green Chem. 2025;9(3):329–54.
21. Dayyih WA, Awad R. Revolutionizing drug development: The role of AI in modern pharmaceutical research. J Pharm Sci Comput Chem. 2025;1(1):206–27.
22. Nagda D, Captain A. Validated Green Densitometric Method for Estimation of Naringin Biomarker in Hydroalcoholic Extract of Leaves of Ceiba Pentandra (L .) Gaertn. Asian J Green Chem. 2025;9:427–42.
23. Abdullah MN, El Arbi M. Silver Nano Loaded Solanum Nigrum with Potential Biological Activities. Chem Methodol. 2024;8(8):585–602.
24. Chandramore KR, Sonawane SS, Ahire RS, Reddy H, Ahire SB, Jadhav PB, et al. Development and Validation of Stability Indicating LC Method for Selexipag : In-Silico Toxicity Study and Characterization of its Degradation Products. Chem Methodol. 2025;9:427–47.
25. Ajeed A, Billah M, Babu RH, D KK, Bubalan K, Bhuvaneshwari G, et al. Phyto-Nanotechnology for Cancer Therapy : A Review of Plant-Mediated Organic Nanoparticles for Targeted Drug Delivery. J Chem Rev. 2025;7(2):131–65.
26. Prinsa, Rana AJ, Saha S, Chaudhary M, Kumar K, Kausar M, et al. Molecular Docking, MD Simulation, Synthesis, DFT, and Biological Evaluations of Newer Generation Imidazolo-Triazole Hydroxamic Acid Linked with Para Nitro Phenyl Group. Adv J Chem Sect A. 2025;8(7):1171–87.
27. Trabelsi R, Yengui M. Green Synthesis of $MgZnFe_2O_4$ Nanoparticles : A Sustainable Approach to Combat β - Lactam-Resistant Uropathogenic Strains. Chem Methodol. 2025;9:489–507.
28. Alabady AA, Al-Majidi SMH. Synthesis, characterization, and evaluation of molecular docking and experimented antioxidant activity of some new chloro azetidine-2-one and diazetine-2-one derivatives from 2-phenyl-3-amino-quinazoline-4(3H)-one. J Med Pharm Chem Res. 2023;5(1):1–18.
29. Ali DN, Ahmed A, Al-Qaisi AHJ. Inhibitory Effect of Newly Prepared Pyrazole Derivatives against Alpha-Amylase in Pancreatic Cancer Cell. Adv J Chem Sect A. 2024;7(3):248–59.

30. Vattikundala P, Chaudhary S, Sumithra M. Design, preparation, characterization, and evaluation of NR4A1 agonist novel 6-mercaptopurine monohydrate loaded nanostructured lipid carriers suspension for enhanced solubility and *in vivo* bioavailability. J Med Pharm Chem Res. 2025;7(6):1059–78.
31. Dolatyari A, Nilchi A, Janitabardarzi S, Alipour A, Hashemi M. Evaluation of Ze/PAN Nanocomposites for Adsorption of Cs (I) from Aaqueous Environments. Chem Methodol. 2025;9(2):103–24.
32. Díaz de los Ríos M, Hernández Ramos E. Determination of the Hansen solubility parameters and the Hansen sphere radius with the aid of the solver add-in of Microsoft Excel. SN Appl Sci. 2020;2(4).
33. Veseli A, Žakelj S, Kristl A. A review of methods for solubility determination in biopharmaceutical drug characterization. Vol. 45, Drug Development and Industrial Pharmacy. 2019. p. 1717–24.
34. Kitak T, Dumičič A, Planinšek O, Šibanc R, Srčič S. Determination of solubility parameters of ibuprofen and ibuprofen lysinate. Molecules. 2015;20(12):21549–68.
35. Abass AM, Abdoon FM. Synthesis, Characterization, and Applications of Metal Oxides of ZnO, CuO, and CeO2 Nanoparticles: A Review. J Appl Organomet Chem. 2024;4(4):349–66.
36. Prasath H, Azhakesan A, Manikandan G. Analytical Methods for Quantification of Gemcitabine in Pharmaceutical and Biological Samples : An Overview of Developments in the Last Decade. Asian J Green Chem. 2025;9:457–75.